

ADSORPTION OF COPPER (II) IONS IN WASTEWATER

USING MANGROVE-BASED ACTIVATED CARBON

BONG SOCK VING

UNIVERSITI SAINS MALAYSIA

2021

ADSORPTION OF COPPER (II) IONS IN WASTEWATER

USING MANGROVE-BASED ACTIVATED CARBON

by

BONG SOCK VING

**Thesis submitted in partial fulfilment of the requirement for the
degree of Bachelor of Chemical Engineering with Honours**

2021

ACKNOWLEDGEMENTS

This final year project is for the completion of degree of Bachelor of Chemical Engineering. Support and commitments from several individuals have contributed to the success in completion of my final year project. Therefore, I would like to show my highest gratitude and appreciation to all the individuals involved for their contribution throughout the project.

First and foremost, I would like to express my sincere appreciation to my supervisor, Associate Professor Dr. Ridzuan Zakaria for his invaluable guidance, insightful supervision and endless encouragement throughout this project. Without the guidance and advice from him, this final year project will not be done entirely on time.

Apart from that, I would like to express my deepest gratitude to my family, fellow friends and coursemates for their endless support and encouragement throughout the time. I would also like to extend my gratitude towards Ms. Tan Kai Qi for her kind ideas and equipment sharing. I would also like to extend my gratitude to all School of Chemical Engineering staff for their kind cooperation, willingness in sharing ideas, knowledge and skills.

Once again, I would like to thank all the people, including those who I might have missed out on mentioning their names but have helped me directly or indirectly in the accomplishment of this project. Thank you very much.

Bong Sock Ving

June 2021

TABLE OF CONTENTS

ACKNOWLEDGEMENTS	iii
TABLE OF CONTENTS	iv
LIST OF TABLES	viii
LIST OF FIGURES	x
LIST OF SYMBOLS	xiv
LIST OF ABBREVIATION.....	xvi
ABSTRAK	xvii
ABSTRACT	xviii
CHAPTER 1 INTRODUCTION	1
1.1 Background.....	1
1.2 Problem Statement.....	2
1.3 Objectives	3
1.4 Thesis Outline	3
CHAPTER 2 LITERATURE REVIEW	5
2.1 Removal of Copper (II) Ions by Adsorption Method.....	5
2.2 Preparation of Activated Carbon	6
2.2.1 Effect of Activation Power	11
2.2.2 Effect of Activation Time	12
2.2.3 Effect of Activation/ Impregnation Agent	14
2.2.4 Effect of Impregnation Ratio (IR).....	16

2.2.5 Mangrove as Raw Materials	18
2.3 Adsorption Isotherm Model	19
2.4 Adsorption Kinetics Model.....	22
2.5 Factor Affecting The Adsorption Performance.....	23
2.5.1 Effect of Contact time.....	24
2.5.2 Effect of Initial Adsorbate Solution Concentration.....	25
2.5.3 Effect of Adsorbate Solution Temperature	27
2.5.4 Effect of Adsorbate Solution pH value	28
2.5.5 Effect of Adsorbent Dosage.....	30
2.6 Summary	31
CHAPTER 3 METHODOLOGY	33
3.1 Research Methodology	33
3.2 Equipment.....	36
3.3 Materials and Chemicals	37
3.4 Optimization of preparation condition for mangrove-based activated carbon.....	37
3.5 Optimization of activating agent.....	39
3.6 Mangrove-Based Activated Carbon Characterisation	40
3.6.1 Textual Surface	40
3.6.2 Functional and Elemental	41
3.7 Preparation of Solutions: HNO ₃ Stock Solution and Copper (II) Solution	41
3.7.1 Nitric Acid, HNO ₃ Stock Solution	42

3.7.2 Copper (II) Solution	43
3.8 Factors Optimization During Adsorption of Copper.....	44
3.8.1 Effect of Contact Time	44
3.8.2 Effect of Initial Adsorbate Solution Concentration.....	44
3.8.3 Effect of Adsorbate Solution Temperature	45
3.9 Adsorption Equilibrium and Isotherm Study	45
3.10 Adsorption Kinetics and Thermodynamics Study	47
CHAPTER 4 RESULTS AND DISCUSSION.....	49
4.1 Optimization on Mangrove-Based Activated Carbon	49
4.1.1 Design Expert: Optimization of Activation Power and Time.....	49
4.1.2 Optimization of Impregnation Ratio of KOH.....	52
4.2 Mangrove-Based Activated Carbon Characterization	53
4.2.1 Textual Surface Analysis.....	53
4.2.2 Functional and Elemental Analysis.....	56
4.3 Effect of Contact Time on Adsorption	60
4.4 Effect of Initial Copper (II) Solution Concentration on Adsorption.....	64
4.5 Effect of Copper (II) Solution Temperature At 10ppm.....	65
4.5.1 Thermodynamics study	66
4.6 Modelling of Adsorption Equilibrium and Isotherm.....	67
4.7 Modelling of Adsorption Kinetics	70
CHAPTER 5 CONCLUSION AND RECOMMENDATIONS	72
5.1 Conclusion.....	72

5.2 Recommendations	73
REFERENCES.....	74
APPENDICES.....	79

LIST OF TABLES

Table 2.1 Comparison of activation technique and maximum adsorption capacity of activated carbon derived from different carbon sources (biomass and wood-based)...	7
Table 2.2 Comparison of activated carbon prepared using conventional and microwave heating.....	10
Table 2.3 Effect of IR on surface characteristics of activated carbon (Hesas <i>et al.</i> , 2013).....	17
Table 2.4 Amount of mangrove forest available in each state of Malaysia (Hamid, 2008).....	19
Table 2.5 Effect of adsorbent dosage on removal percentage and adsorption capacity at 100 ppm adsorbate concentration (Aydin, Bulut and Yerlikaya, 2008).....	31
Table 3.1 List of materials and chemicals required and their purpose.....	37
Table 3.2 Purpose of the equipment required.....	36
Table 3.3 Factor and coded variable levels for CCD.....	38
Table 3.4 Dependents factors (responses).....	38
Table 3.5 Experimental design matrix generated by Design Expert.....	40
Table 3.6 Weight of KOH required at different IR.....	40
Table 3.7 Volume of each solution required to prepare various concentration of copper (II) solution.....	43
Table 3.8 Volume of each solution required to prepare various concentration of copper (II) solution.....	45
Table 4.1 Factors and responses for Central Composite Design in Design Expert.....	50
Table 4.2 Activated carbon yield and copper (II) ion removal at different IR of KOH.....	52

Table 4.3 Structural characteristics of mangrove char, unmodified AC and KOH modified AC.....	54
Table 4.4 FTIR peak intensity analysis of unmodified and KOH impregnated AC....	58
Table 4.5 Elemental analysis of mangrove char, unmodified activated carbon and KOH impregnated activated carbon.....	60
Table 4.6 Isotherm parameters for the adsorption of copper (II) ions.	68
Table 4.7 Kinetics model parameters for the adsorption of copper (II) ions.	70

LIST OF FIGURES

Figure 2.1 Effect of activation power on wood sawdust activated carbon yield and adsorption uptake (Foo and Hameed, 2012b).	11
Figure 2.2 Effect of microwave power on sunflower seed husks activated carbon surface area (Baytar, Şahin and Saka, 2018).	11
Figure 2.3 Effect of activation time on the BET surface area, pore volume and yield percentage of activated carbon (Shoaib and Al-Swaidan, 2015).	13
Figure 2.4 Effect of activation time on activated carbon yield and adsorption uptake (Foo and Hameed, 2012a, 2012b).	13
Figure 2.5 Effect of activation agent on activated carbon yield and adsorption uptake (Foo and Hameed, 2012a).	15
Figure 2.6 Effect of IR (a) KOH (Foo and Hameed, 2012a), (b) K ₂ CO ₃ (Foo and Hameed, 2012b) on activated carbon yield and adsorption uptake.	17
Figure 2.7 Area where mangrove forest can be found in Malaysia in 2017 (Omar, Husin and Parlan, 2020).	19
Figure 2.8 Types of isotherms defined by IUPAC (Nishi and Inagaki, 2016).	20
Figure 2.9 Effect of contact time on removal efficiency of Fe ²⁺ , Pb ²⁺ and Cu ²⁺ ions onto olive stone activated carbon (Alslaibi <i>et al.</i> , 2014).	24
Figure 2.10 Effect of contact time on removal efficiency of Cu (II) ions at different initial concentration onto sugarcane bagasse activated carbon (Salihi, Kutty and Ismail, 2018).	24
Figure 2.11 Effect of contact time on Cu (II) and Ni (II) adsorption onto modified mangrove barks activated carbon (Rozaini <i>et al.</i> , 2010).	25
Figure 2.12 Effect of initial dye concentration on the adsorption capacity (Foo and Hameed, 2012b).	26

Figure 2.13 Effect of initial heavy metal solution concentration on metal removal percentage (Rozaini <i>et al.</i> , 2010).	26
Figure 2.14 Effect of initial heavy metal concentration on metal Pb (II) and Zn (II) removal percentage (Marda and Astuti, 2017)	27
Figure 2.15 Effect of adsorbate solution temperature on heavy metal adsorption onto corn straw (CS) and hardwood (HW) (Chen <i>et al.</i> , 2011).	28
Figure 2.16 Effect of pH on removal efficiency of heavy metals onto mangrove activated carbon (Marda and Astuti, 2017).	29
Figure 2.17 Effect of pH on removal efficiency of Cu ²⁺ onto different activated carbon (LS: Lentil shell; WS: Wheat shell; RS: Rice shell) (Aydin <i>et al.</i> ,2008).	29
Figure 2.18 Effect of pH on the adsorption MB onto activated carbon (Foo and Hameed, 2012b).	29
Figure 2.19 Effect of adsorbent dosage on the heavy metal removal (Rozaini <i>et al.</i> , 2010).	30
Figure 3.1 Flow diagram of research project on optimization and adsorption.	33
Figure 3.2 Set-up of microwave oven with nitrogen gas flow.....	34
Figure 3.3 Position of tube A and tube B.....	35
Figure 3.4 Set-up of test tube inside the microwave.....	35
Figure 3.5 Grinded mangrove pieces from mangrove stem.....	39
Figure 4.1 Summary of desirability optimization result of radiation power, radiation time, Cu ²⁺ removal and AC yield by Central Composite Design.	50
Figure 4.2 Desirability optimization of AC yield based on different combination radiation power and time by CCD.	51
Figure 4.3 Desirability optimization of different combination radiation power and time by CCD.	51

Figure 4.4 Effect of Impregnation ratio of KOH on AC yield and copper (II) ions removal.	52
Figure 4.5 Nitrogen adsorption/desorption isotherm of unmodified mangrove-based AC.	53
Figure 4.6 Nitrogen adsorption/desorption isotherm of KOH impregnated mangrove-based AC.	54
Figure 4.7 FTIR spectra of unmodified mangrove-based AC.	56
Figure 4.8 FTIR spectra of KOH impregnated mangrove-based AC.	57
Figure 4.9 Effect of contact time on copper (II) ions removal using mangrove nased AC at different temperature.	61
Figure 4.10 Effect of contact time on equilibrium adsorption uptake using mangrove nased AC at different temperature.	61
Figure 4.11 Effect of contact time on copper (II) ion removal using magrove based AC at various concentration at 60°C.	63
Figure 4.12 Effect of initial copper (II) ions concentration on ions removal percentage and adsorption uptake.	64
Figure 4.13 Effect of temperature on Gibb’s free energy of the copper (II) ions adsorption using mangrove based AC.	66
Figure 4.14 Langmuir isotherm fitting of 10ppm of copper (II) solution at 40°C.	67
Figure 4.15 Freundlich isotherm fitting of 10ppm of copper (II) solution at 40°C.	67
Figure 4.16 Langmuir isotherm fitting of 10ppm of copper (II) solution at 50°C.	67
Figure 4.17 Freundlich isotherm fitting of 10ppm of copper (II) solution at 50°C.	67
Figure 4.18 Langmuir isotherm fitting of 10ppm of copper (II) solution at 60°C.	68
Figure 4.19 Freundlich isotherm fitting of 10ppm of copper (II) solution at 60°C.	68

Figure 4.20 Pseudo 1st order kinetics fitting of 10ppm of copper (II) solution. 70

Figure 4.21 Pseudo 2nd order kinetics fitting of 10ppm of copper (II) solution. 70

LIST OF SYMBOLS

Symbol	Description	Unit
$1/n$	Heterogeneity factor	-
C_1	Concentration of stock solution	M or ppm
C_2	Final concentration after dilution	M or ppm
C_e	Equilibrium metal ion concentration after adsorption	ppm or mg/L
C_o	Initial metal ion concentration	ppm or mg/L
K	Langmuir equilibrium coefficient	L/mg
K_e	Adsorption equilibrium constant	L/g
K_F	Freundlich constant	L/mg
k_1	Rate constant of PFO kinetic	min^{-1}
k_2	Rate constant for PSO adsorption kinetic	g/mg. min
M	Amount of adsorbent	g
q_e	Amount of metal ion uptake/Adsorption equilibrium	mg/g
q_{\max}	Maximum adsorption capacity	mg/g
q_t	Adsorption capacity taken at time	$\text{mg/g}_{\text{adsorbent}}$
R	Gas constant	J/mol. K
T	Absolute temperature	K
t	Time taken to reach equilibrium	min
V_1	Volume of stock solution required	mL or L
V_2	Final volume of diluted solution	mL or L
W	Watt (unit of power)	-
ΔG°	Standard Gibbs free energy	J/mol
ΔH°	Standard enthalpy	J/mol
ΔS°	Standard entropy	J/mol

Greek letter

α Selectivity/ Separation factor -

LIST OF ABBREVIATION

Symbol	Description
AAS	Atomic Absorption Spectrometer
AC	Activated Carbon
BET	Brunauer–Emmett–Teller
CCD	Central Composite Design
CHNS	Carbon Hydrogen Nitrogen Sulphur
FTIR	Fourier Transform Infrared
IR	Impregnation Ratio
IUPAC	International Union for Pure and Applied Chemistry
MW	Molecular Weight
PFO	Pseudo-First-Order
PSO	Pseudo-Second-Order
R ²	Correlation Coefficient
RSM	Response Surface Methodology
SEM	Scanning Electron Microscope
Δq	Normalized Standard Deviation of Adsorption Capacity

PENJERAPAN ION KUPRUM (II) DARI AIR SISA DENGAN KARBON TERAKTIF DARIPADA BATANG BAKAU

ABSTRAK

Pencemaran air berpunca daripada pembuangan air yang terdiri daripada logam berat telah menjadi isu yang serius. Bahan penjerap yang murah diperlukan untuk menyokong teknik penjerapan bahan pencemar. Oleh itu, tujuan utama penyelidikan ini adalah untuk mengoptimumkan keadaan penyediaan dan penjerapan sesuatu karbon teraktif dari bahan mentah yang murah. Penghasilan karbon teraktif dengan menggunakan pemanasan gelombang mikro dari kayu bakau adalah salah satu kaedah yang paling menjimat wang kerana bakau boleh didapati di Malaysia dan pemanasan gelombang mikro memerlukan jangka masa yang lebih pendek dan penggunaan elektriknya lebih rendah. Karbon teraktif yang paling optimum dihasilkan pada 616 W dan 2 minit dengan aliran nitrogen. Selain itu, nisbah KOH: Char yang terbaik adalah pada IR 0.75 dengan 99.67% penghasilan karbon teraktif dan 77.256% ion kuprum (II) telah dijerapkan. Karbon teraktif telah diperiksa dengan Spektroskopi Inframerah Jelmaan Fourier, Isoterma penjerapan nitrogen dan analisis unsur. Selain pengoptimuman, proses penjerapan yang menggunakan bahan penjerap kayu bakau diperiksa dalam pelbagai keadaan. Dari data eksperimen, penjerapan mencapai keseimbangan setelah 3 pada 10 ppm dan 60°C. Model isotherm *Freundlich* dengan nilai $R^2 = 0.9995$ dan nilai $1/n$ kurang daripada 1 telah mewakili data eksperimen ini. Kapasiti penjerapan tertinggi ialah 33.557 mg/g. Selanjutnya, data tersebut juga sesuai dengan model kinetika *Pseudo-Second-Order* dengan nilai $R^2 = 0.9997$ dan kapasiti penjerapan maksimum 8.4746 mg/g. Akhirnya, analisis termodinamik menunjukkan bahawa pada suhu 50 dan 60 ° C, penjerapan dalam kajian ini adalah spontan.

ADSORPTION OF COPPER (II) IONS IN WASTEWATER USING MANGROVE-BASED ACTIVATED CARBON

ABSTRACT

Water pollution due to the discharging of industrial wastewater consisting of heavy metals has become a serious issue. A cheap adsorbent is required to support the pollutant adsorption technique. Thus, the main goal of the research is to optimise the preparation and adsorption conditions of activated carbon from cheap raw materials. The production of mangrove-based activated carbon using microwave heating activation is cost-effective because mangrove is abundantly available in Malaysia and microwave heating requires less time and lower electricity. The optimal activated carbon was produced at 616 W and 2 mins under nitrogen flow. The ideal KOH: Char ratio was found to be at IR of 0.75 with 99.67% of activated carbon yield and 77.256% of copper (II) ions removal. The AC was examined by Fourier transform infrared spectroscopy, nitrogen adsorption/desorption isotherm and elemental analysis. Aside from optimisation, the adsorption process using the mangrove adsorbent was examined under various conditions. From the experimental data, the adsorption reached equilibrium after 3 hours at 10ppm and 60°C. Freundlich isotherm models with R^2 values of 0.9995 and $1/n$ smaller than one explains the multilayer and heterogenous nature of adsorption. The maximum adsorption capacity of mangrove-based activated carbon obtained using Langmuir Isotherm was 33.557 mg/g, which shows its intrigue value as a potential adsorbent. Furthermore, the data was well fitted to Pseudo-second-order kinetics models with R^2 value of 0.9997. Finally, the thermodynamic analysis revealed that the adsorption studied is endothermic process, and the adsorption is spontaneous at 50 and 60°C.

CHAPTER 1

INTRODUCTION

Chapter 1 introduces the overview of this research and summarises the research background of heavy metal, the problem statement, the objective and the outline of this project.

1.1 Background

The most common heavy metals present in the industry are Copper (Cu), Chromium (Cr), Cadmium (Cd), Iron (Fe), Lead (Pb), Nickel (Ni), Zinc (Zn), and Arsenic (As). These heavy metals are used for the production of colour pigments of textile dyes (Bhardwaj, Kumar and Singhal, 2014). The copper (II) ions found are between 0.17 – 0.28 mg/L. Besides, in the pulp and paper mill industry, Copper (Cu), Manganese (Mn), Chromium (Cr), Iron (Fe), Cadmium (Ca), Nickel (Ni), Lead (Pb) are found in the wastewater (Mandeep *et al.*, 2019).

Moreover, Buhari and Ismai (2020) discuss on the serious heavy metals (Cu, Zn, Pb, Cd, and Ni) pollution in the surface sediments of the west coast in Malaysia. The sampling site studied were Kuala Juru, Sungai Puluh, Bagan Lalang, Minyak Beku and Sungai Tiga. All the sampling sites were jetty, industrial, and agricultural area. It is reported that more than 700 organic and inorganic pollutants have been found in the watercourse of the sampling sites. Among these pollutants, heavy metal ions are the most dangerous pollutant due to their toxic and carcinogenic properties. Additionally, some heavy metal ions are non-biodegradable and non-transformable (Ali, 2010).

Copper is a heavy metal pollutant typically found in water pollution. It is an essential enzyme cofactor that is always supplied for human growth and development.

However, copper in a compound form such as copper sulphate is harmful to human respiratory system, leading to gastrointestinal anaemia, multiple destructions of the capillaries, liver, and kidney dysfunction (Ugwu and Agunwamba, 2020). The main sources of its contamination are wastewater from agricultural fields and industrial areas like electrical, metal finishing, paint, electroplating, pigment, and wood manufacturing industries (Ali, 2012).

1.2 Problem Statement

Based on Environmental Quality Act 1974: Environmental Quality (Sewage And Industrial Effluents) Regulations 1979, the maximum concentration of copper ions discharged for standard A is 0.2 mg/L and 1.0mg/L for standard B, where standard A is where the discharge point is at the upstream of a water intake point for consumption or water catchment areas and standard B is applied if the point of discharge into the water catchment area (Malaysia Government, 1979). Therefore, it is necessary to remove copper from wastewater before it is discharged into any water source.

Different water purification technologies are available to remove copper (II) ions in wastewater, for example, reverse osmosis, ion exchange, electro dialysis, electrolysis, filtration, adsorption, and centrifugation. However, the cost of these current technologies available, except adsorption, ranges from 10 to 450 USD (RM 40.41 to RM1818.22) per cubic meter of water. On the other hand, the cost required for adsorption operation using activated carbon is 5 to 200 USD (RM 20.20 to RM 808.10) per cubic meter of water (Ali, 2010).

However, significant amount of adsorbent is required to remove the heavy metal in high volume of wastewater, leading to high expenditure of money. Activated

carbon is a suitable adsorbent for the adsorption of heavy metals because it has small particle sizes and active free valences, which provide a good adsorption capacity. Furthermore, due to the simplicity of preparation and regeneration, adsorption using activated carbon appears to be the most common technique. Therefore, it is essential to discover a low-cost alternative raw material and heating technique to synthesize the activated carbon. In this project, the low-cost raw material chosen is the mangrove stem and the cheaper heating technique is microwave-heating. The characteristics and adsorption performance of the produced activated carbon were also studied.

1.3 Objectives

The research work in this thesis is performed to achieve the objectives as listed below:

- i. To investigate the factors that affect the characteristics of mangrove-based activated carbon.
- ii. To study the factors that affect the copper (II) ions adsorption efficiency onto mangrove-based activated carbon.
- iii. To determine the adsorption isotherm of copper (II) ions adsorption using mangrove-based activated carbon.
- iv. To investigate the adsorption kinetics of copper (II) ions adsorption using mangrove-based activated carbon.

1.4 Thesis Outline

There are five main chapters in this thesis. The following are the contents of each chapter in this study: **Chapter 1 Introduction** briefly introduces the overview of this research and summarises the research background of heavy metal, the problem statements, the objective and the outline of this thesis. Next, **Chapter 2 Literature review** presents the previous studies and reviews available from scientists and

researchers related to this topic. This chapter covers the activated carbon preparation, adsorption isotherm, adsorption kinetics and adsorption performance. Factors that influence the activated carbon pore distribution and adsorption capacity are discussed in the chapter. **Chapter 3 Methodology** covers the general research flow diagram, methodology details on activated carbon optimization, materials, equipment and copper (II) ions adsorption experiment. Moreover, **Chapter 4 Results and discussion** covers the outcomes of mangrove-based activated carbon optimisation and copper (II) ion adsorption experiments. Ideal activated carbon preparation and adsorption conditions are suggested and reviewed based on the experimental results. Lastly, **Chapter 5 Conclusion and recommendations** covers a summary of the experiment data and recommendation for future researchers.

CHAPTER 2

LITERATURE REVIEW

Chapter 2 presents the previous discoveries and reviews available from credible scientific records and references related to this project. In addition, this chapter covers the overview of activated carbon preparation and adsorption performance.

2.1 Removal of Copper (II) Ions by Adsorption Method

Adsorption using activated carbon is a surface phenomenon in which the pollutants are adsorbed on the solid surface of activated carbon. The pollutants that adhere to the solid surface are called adsorbate, and the solid surface is known as adsorbent. Adsorption is influenced by various parameters like the nature of the adsorbate and adsorbent, and the presence of other pollutants and the experimental conditions such as contact time, pH and concentration of adsorbate solution, temperature of solution, and adsorbent dosage. The adsorption mechanism is commonly described using the isotherm models, and the limiting rate is determined using the kinetics model. In addition, thermodynamics properties of the adsorption process are also studied by changing the temperature of the adsorbate solution.

Recent studies show different carbon sources used to synthesize activated carbon for copper (II) ions adsorption in industrial wastewater treatment. In Table 2.1, there are different activated carbon prepared from different raw materials and activation techniques for the Cu (II) ions adsorption. Based on their characteristics and best operating conditions as decided by the researchers, their maximum adsorption capacities (mg/g) on Cu (II) ions from their best-fit isotherm model are also shown in the table. Chemical activation was done using different heating techniques: microwave and conventional. The conventional heating method was carried out in a furnace at different temperature (around 400-600°C) for more than 30 min under

nitrogen flow. While microwave heating was performed in a microwave oven with the microwave activation power and time based on the capability of the microwave in the range of less than 30 min.

Table 2.1 shows that both biomass and wood-based activated carbon can be prepared using either conventional or microwave heating. For conventional heating technique, the highest Q_{\max} obtained was 90.90mg/g using modified cassava tuber bark (wood based) whereas modified mangrove stem in present project obtained the highest Q_{\max} of 33.56mg/g for microwave heating technique. Besides, by comparing the Q_{\max} of microwave-heated and conventional-heated modified olive stone, it was shown that microwave-heated olive stone (22.73mg/g) has a higher Q_{\max} than that by conventional heating (17.83mg/g) (Alslaibi *et al.*, 2014).

2.2 Preparation of Activated Carbon

Activated carbon is usually produced by carbonization at high temperatures with an inert atmosphere, followed by the activation process. The activation process is a significant step where it will influence the characterisation of the activated carbon produced, leading to a different performance of adsorption. The porous surface is usually created during the activation process. There are two types of activation process: physical and chemical activation. The physical activation process involved treatment of char obtained from carbonization with oxidizing gases such as steam or carbon dioxide at elevated temperature. The pores formed during carbonization are filled with pyrolysis residues; hence, activation is required to increase the internal surface of the activated carbon (Hidayu and Muda, 2016).

Table 2.1 Comparison of activation technique and maximum adsorption capacity of activated carbon derived from different carbon sources (biomass and wood-based).

Activation technique	Source	Max. adsorption capacity, Q_{max} (mg/g)	Ref.
Conventional	Chitosan	43.47	(Kannamba <i>et al.</i> , 2010)
	Lentil shell	9.59	
	Rice shell	2.95	(Aydin <i>et al.</i> , 2008)
	Wheat shell	17.42	
	Black carrot	8.88	(Güzel, Yakut and Topal, 2008)
	Soybean straw	48.14	(Zhu, Fan and Zhang, 2008)
	<i>Agaricus bisporus</i>	11.44	(Ertugay and Bayhan, 2010)
	<i>Ceiba pentandra</i> hulls	20.80	(Madhava Rao <i>et al.</i> , 2006)
	Modified olive stone	17.83	(Alslaibi <i>et al.</i> , 2014)
	Sugarcane bagasse	0.45	(Salihi, Kutty and Ismail, 2018)
	Corn straw	12.52	
	Hardwood	6.79	(Chen <i>et al.</i> , 2011)
	Modified cassava tuber bark	90.90	(Horsfall, Abia and Spiff, 2006)
	Modified oakwood sawdust	3.22	(Argun <i>et al.</i> , 2007)
	Modified mangrove Barks (<i>Rizophora apiculate</i>)	5.80	(Rozaini <i>et al.</i> , 2010)
Microwave	Bagasse	25.12	(Wan and Li, 2018)
	Modified sewage sludge	10.56	(Wang <i>et al.</i> , 2011)
	Modified olive stone	22.73	(Alslaibi <i>et al.</i> , 2014)
	Modified mangrove stem	33.56	Present work

In the chemical activation process, an activation reagent such as $ZnCl_2$, H_3PO_4 , H_2SO_4 , KOH , and $NaOH$ mixes with the raw material and the mixture is heated in an inert atmosphere. Different activating agents are used to give the different size of pores. Moreover, the temperature and time for activation are the most important factors that control the final pore structure, surface area, and the chemistry of the carbon prepared.

Activation is commonly carried out using conventional heating. However, Hesas *et al.* (2013) and Marda and Astuti (2017) show that conventional heating is high energy, time, and money consumption. Based on both pieces of research, during conventional heating, the heat source is located outside the carbon bed, and energy is transferred to the sample to be activated from the inward surface to its interior by convection, conduction, and radiation. As a consequence, there is a thermal gradient between the hot activated carbon surface and its interior. This thermal gradient precludes the release of gaseous products like pyrolysis gas to the surrounding atmosphere and leads to uniform heat distribution since some volatile components may remain in the activated carbon. The heating rate is reduced and the activation process is lengthened to eliminate the temperature gradient and reach the desired temperature. A longer duration of heating will undoubtedly increase the cost and energy consumption.

On the other hand, microwave heating is also applicable for activation. Microwave heating is conducted inside a microwave oven with a different range of radiation power and time, allowing inert gas flow like nitrogen into the raw materials to be activated. An activating agent is still required for impregnation in order to improve the pore distribution in the activated carbon produced. Recently, researchers have proposed microwave heating technique as an alternative to replace conventional

heating in creating activated carbon for dye removal. As compared to conventional heating, microwave heating produces activated carbon which performs better in adsorption in a shorter activation time and thus reduces energy usage and cost. As discussed by Baytar, Şahin and Saka (2018), Marda and Astuti (2017) and Alslaibi *et al.* (2014), in microwave heating, the microwave energy can be easily transformed into heat and transferred inside the particles via dipole rotations and ionic conduction, resulting in a tremendous temperature gradient that steadily decreases from the interior of the sample to its surface bulk. This temperature gradient allows the microwave-induced reaction to proceed more aggressively and effectively at a low bulk temperature, causing the partial breakdown of volatile compounds during the activation process.

Table 2.2 below shows the comparison of activated carbon prepared using conventional and microwave heating. According to the comparison, it can be observed that microwave heating uses a much shorter duration for activation as compared to conventional heating, but it still results in a comparable activated carbon with higher adsorption capacity. Higher adsorption capacity indicates a better adsorbate removal effectiveness. From the table, a lower BET surface area is due to the pore distribution which can be estimated from the average pore size. There are three types of pores, namely micropores (< 2 nm), mesopores (2 and 50 nm), and macropores (> 50 nm). Organic substances are decomposed into volatile gases and liquid tar due to high-temperature pyrolysis operations and the disposal of tar and volatile compounds to the environment is accelerated compared to conventional heating, resulting in activated carbon with higher carbon content (Hesas *et al.*, 2013).

Table 2.2 Comparison of activated carbon prepared using conventional and microwave heating.

Raw material	Activation technique	Activating agent	Operating conditions	BET surface area (m ² /g)	Average Pore Size (nm)	Adsorption capacity (mg/g)	Ref
Oil palm shell	Conventional	ZnCl ₂	500 °C; 120 min	1672.00	0.236	N/A	(Hesas <i>et al.</i> , 2013)
	Microwave		1050 W; 15 min	1195.00	0.217	N/A	
Bagasse	Conventional	HNO ₃ + H ₂ SO ₄	500 °C; 90 min	609.00	3.840	12.00	(Wan and Li, 2018)
	Microwave		900 W; 22 min	61.00	8.890	16.00	
Olive stones	Conventional	KOH	715 °C; 120 min	886.72	4.220	17.83	(Alslaibi <i>et al.</i> , 2014)
	Microwave		565 W; 7 min	1280.71	4.630	22.73	

2.2.1 Effect of Activation Power

For microwave heating, activation power is as important as activation temperature. Studies from Foo and Hameed (2012a, 2012b) and Baytar, Şahin and Saka (2018) indicated a similar trend for this parameter. The studies by Foo and Hameed (2012a, 2012b) were both carried out for 5 min and power of 90 to 800 Watt while the other was done at 200 to 1000Watt and 30 min.

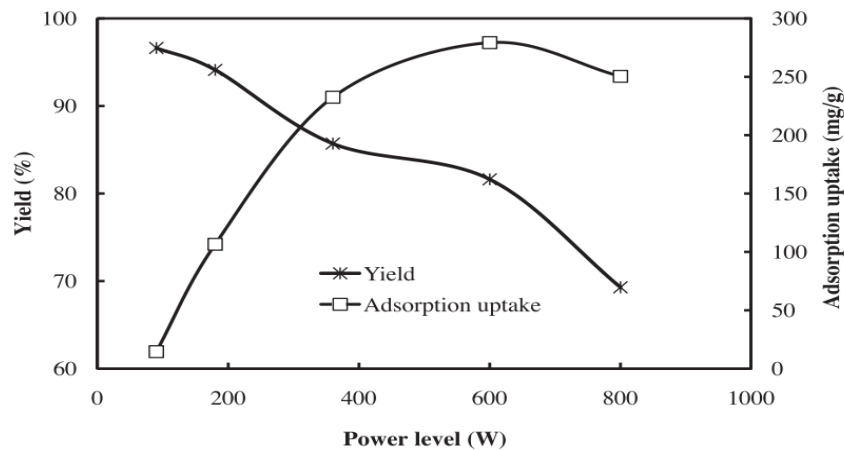


Figure 2.1 Effect of activation power on wood sawdust activated carbon yield and adsorption uptake (Foo and Hameed, 2012b).

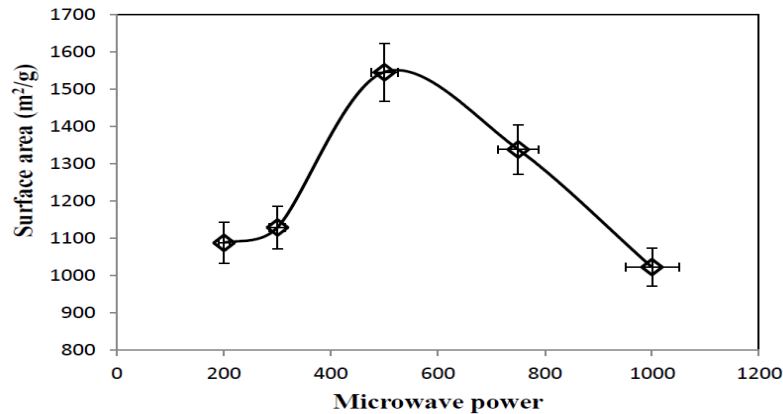


Figure 2.2 Effect of microwave power on sunflower seed husks activated carbon surface area (Baytar, Şahin and Saka, 2018).

In Figure 2.1, at a power level less than 180 W, the activated carbon yield and adsorption uptake remained constant, showing no ongoing reaction between the char and activation agent. Whereas from 180 to 800W, a drastic decrease in activated carbon yield was due to the weight loss of carbon. This weight loss of carbon also

increased proportional to the microwave power, mainly because of the harsh response at higher thermal radiation which accelerate the devolatilization, dehydration, and decomposition (Foo and Hameed, 2012a, 2012b).

At the same time, a drastic increase in adsorption uptake was observed when activation power was increased from 180 to 600W as shown in the Figure 2.1. This sharp increase in adsorption uptake possibly attributed to the combined effect of internal and volumetric heating which causes the carbon structure to expand and create high porosity and a larger surface area (Foo and Hameed, 2012a). This can be proven by the study from Baytar, Şahin and Saka (2018) as shown in Figure 2.2. From 200 to 600W, the surface area of the activated carbon prepared increased from 1088 to 1511m²/g.

Moreover, at radiation power more than 600W, over gasification might occur with the second break down of the uncompensated gases, which lead to the detrimental effect of reducing surface area and excessive degradation of pore structures (Foo and Hameed, 2012a, 2012b; Baytar, Şahin and Saka, 2018); thus, the adsorption uptake, carbon yield and surface area were progressively decreased.

2.2.2 Effect of Activation Time

Activation time is also another significant factor that will affect the surface area and yield of activated carbon. Based on Shoaib and Al-Swaidan (2015), a longer activation time until an optimum value increased the pore volume and surface area.

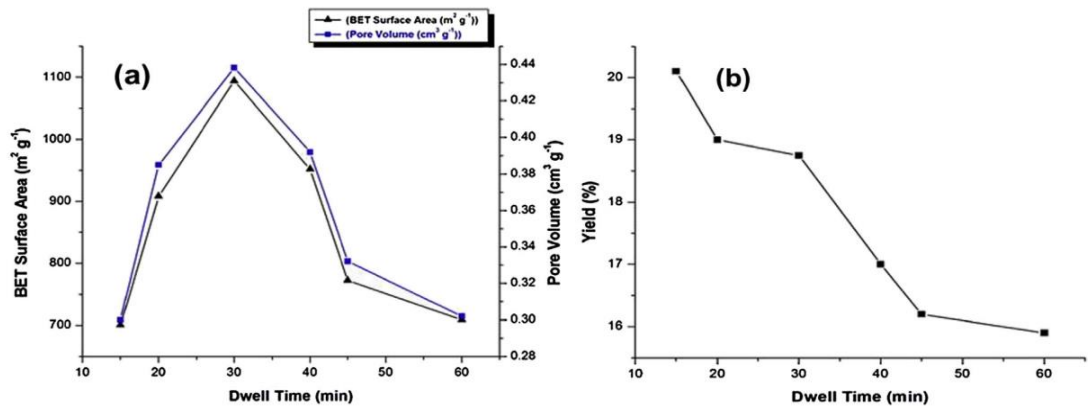


Figure 2.3 Effect of activation time on the BET surface area, pore volume and yield percentage of activated carbon (Shoaib and Al-Swaidan, 2015).

Figure 2.3 shows the effect of activation time on the BET surface area, pore volume, and yield percentage of activated carbon. As shown in the figure, when activation time increased from 15 to 30 min, the pore volume and BET surface area of activated carbon increased. At 30 min, the BET surface area ($1094\text{m}^2/\text{g}$) and pore volume ($0.4382\text{cm}^3/\text{g}$) of activated carbon were the highest with a moderate yield of activated carbon (18.75%).

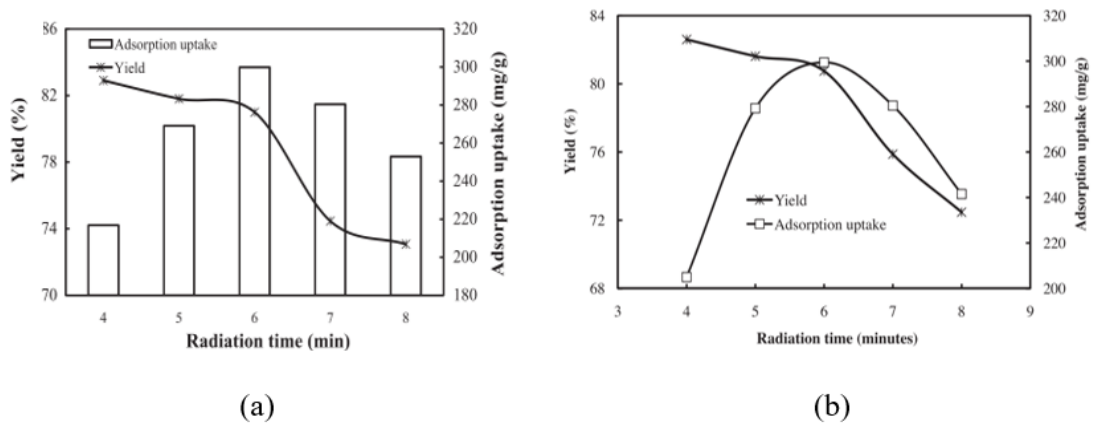


Figure 2.4 Effect of activation time on activated carbon yield and adsorption uptake (Foo and Hameed, 2012a, 2012b).

Similarly, Foo and Hameed (2012a, 2012b) also explored the effect of activation time on the activated carbon yield and adsorption uptake. Both studies revealed similar trend of adsorption uptake and activated carbon yield. When the activation time increased from 2 to 6 min, adsorption uptake increased as well. The

highest adsorption uptake was recorded at 6 min, while the maximum yield percentage was at 4 min. At 6 min, the yield percentage was moderate and comparable. Hence, it was the recommended optimal activation time.

From Figure 2.3 and Figure 2.4, sharp decline of BET surface area, yield and adsorption uptake was observed when the time was further prolonged. It was most likely due to a sintering effect, which significantly degraded the pore walls between neighbouring pores and widens the micropores and mesopores, causing exterior shrinkage and collapse of the carbon framework (Foo and Hameed, 2012b). Furthermore, longer time stimulated the reaction between carbon and activation agents or volatile gas, promoting the breakdown of the C-O-C and C-C bonds and lowering the activated carbon yield (Foo and Hameed, 2012a).

2.2.3 Effect of Activation/ Impregnation Agent

In the study by Foo and Hameed (2012a), activation agents used during the activation has significantly influenced the activated carbon yield and adsorption uptake. By adding an activating agent, pore width was gradually increased and new micropores were produced in the original pore walls, leading to a subsequent increase in BET surface area and pore volume. In the study, H_2SO_4 , H_3PO_4 , HNO_3 , K_2CO_3 , $NaOH$, and KOH were added with the same impregnation ratio of 1:1. Different activation agents resulted different activated carbon yield and adsorbate removal at the same operating conditions.

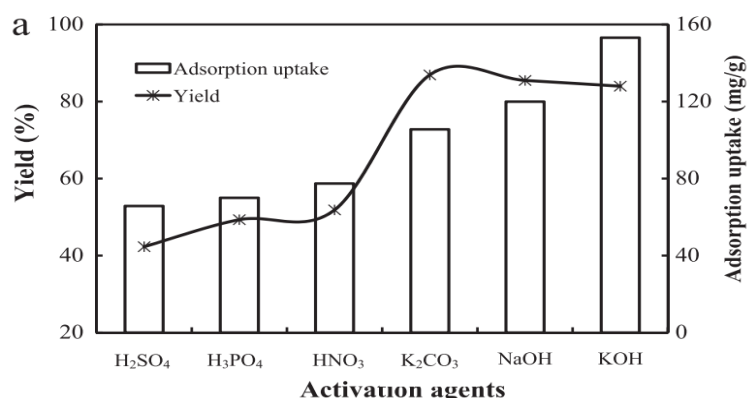
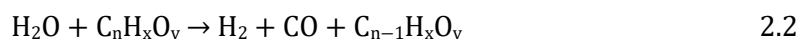
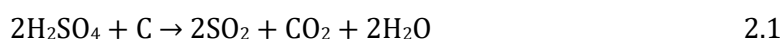


Figure 2.5 Effect of activation agent on activated carbon yield and adsorption uptake (Foo and Hameed, 2012a).

In Figure 2.5, K₂CO₃ gave the highest percentage of activated carbon yield (85%), whereas KOH resulted activated carbon that has the highest adsorption uptake at 96 mg/g. H₂SO₄ was considered as the least recommended activation agent since it produced the least activated carbon and lowest adsorption uptake. When sulphuric acid reacted with carbon in char, it introduces oxygen functionalities by the reaction as shown in Eq. 2.1. The key problem was that the water vapour generated spontaneously depleted the carbon content in the activated carbon as described in Eq. 2.2.



Moreover, K₂CO₃ is a good activation agent to yield the highest activated carbon but the adsorption capacity is moderate. Reduction of K₂CO₃ produces K, K₂O, CO, and CO₂. The potassium compound generated able to penetrate the interior structure of the char surface, widening the existing pores (Foo and Hameed, 2012b). Next, KOH and NaOH are both alkaline hydroxide activation agents. Porosity is developed through redox reduction and carbon oxidation during alkaline hydroxide activation. Metallic potassium formed during the redox reaction of KOH, similar to that from K₂CO₃, can be intercalated into the matrix independently for separation and degradation of carbon layers, resulting in the development of the micro and mesopores.

In contrast, sodium can only intercalate in highly defective materials. It explained the variation between adsorption uptakes of activated carbons produced using KOH and NaOH, despite their yield percentages being similar. In short, the activated carbon produced using KOH and NaOH as the activation agent was recommended with the high adsorption uptake and comparable yield.

2.2.4 Effect of Impregnation Ratio (IR)

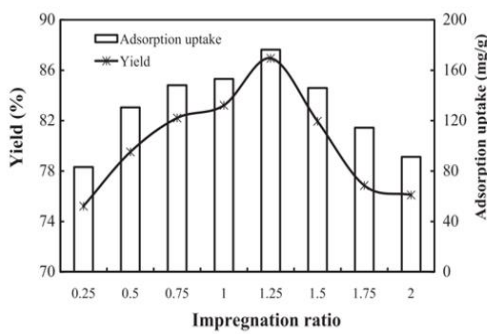
Apart from selecting the best activation agent, the impregnation ratio (IR) also influences the activated carbon characteristics and adsorption efficiency. IR is defined as the dry weight of the activation agent per weight of char as described in Eq. 2.3.

$$IR = \frac{W_{activation\ agent}}{W_{char}} \quad 2.3$$

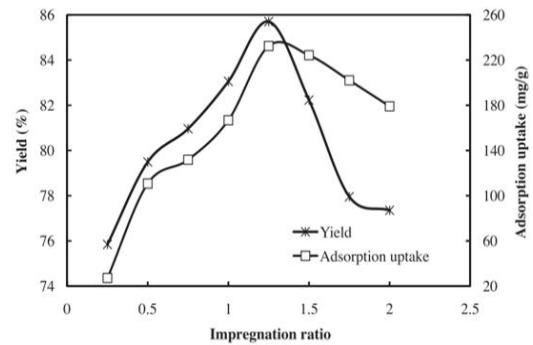
Based on the study from Hesas *et al.* (2013), it was concluded that 0.65 is optimal for ZnCl₂ to produce palm shell activated carbon using microwave activation. In Table 2.3, raising the IR from 0.15 to 0.65 had gradually increased the S_{BET} of the prepared activated carbon to 1195 m²/g. The increase of S_{BET} was due to the creation of micropores and mesopores during the activation process. Furthermore, Table 2.3 also illustrates the continuously increasing trend of average pore size and total pore volume with increasing IR. When the IR was increased further to 0.90, the S_{BET} subsequently decreased to 1079 m²/g. Some of the micropores were slowly being widened and merged into mesopores at higher IR. Excessive activation agent also degrade or clog some of the micropores. After the optimal amount of activating agent was used for the pore development, there was high possibility that a layer of the remaining amount of activating agent forming on the pore surface of the activated carbon or block inside the pores. Thus, the diffusion of adsorbate into the interior surface of the activated carbon for adsorption was restricted.

Table 2.3 Effect of IR on surface characteristics of activated carbon (Hesas *et al.*, 2013).

IR	S _{BET} (m ² /g)	Average pore size (nm)	Total pore volume (cm ³ /g)
0.15	443	2.04	0.23
0.28	622	2.06	0.32
0.40	738	2.14	0.39
0.53	860	2.15	0.46
0.65	1195	2.17	0.65
0.78	1137	2.26	0.68
0.90	1079	2.43	0.70



(a)



(b)

Figure 2.6 Effect of IR (a) KOH (Foo and Hameed, 2012a), (b) K₂CO₃ (Foo and Hameed, 2012b) on activated carbon yield and adsorption uptake.

In 2012, Foo and Hameed (2012a, 2012b) had investigated the IR of KOH to coconut husk and K₂CO₃ to wood sawdust char. According to Figure 2.6, both investigations concluded that 1.25 ratio was the best IR among the range of 0.25 to 2.00 with the highest activated carbon yield (%), and adsorption uptake (mg/g). Beyond 1.25 IR, the subsequent increase in IR reflected a progressive decline in activated carbon yield and adsorption uptake. From the different optimal IR for different agent, a hypothesis can be made: there is no best IR value can be suggested for every impregnation agent.

The drastic decrease in carbon yield and adsorption uptake was explained by the excessive activation agent such as ZnCl₂, KOH, and K₂CO₃ blocks the pores and disrupts the carbon framework in the char. Besides, excessive activation agent like

KOH decomposed to form water vapours which will react with carbon in the char as shown in Eq. 2.4 and 2.5 (Foo and Hameed, 2012a). The vigorous reaction led to a dramatic decrease of carbon content in activated carbon and reduced the BET surface area.



2.2.5 Mangrove as Raw Materials

Rather than saving money during preparation by applying a better activation condition, as previously discussed, another point of interest is the synthesis of activated carbon from a low-cost carbon source raw material such as mangrove, which is readily available in Malaysia.

Mangrove stem is abundantly available in brackish water areas in Malaysia. There are 110,953 hectares in Peninsular Malaysia, 139,890 hectares in Sarawak and 378,195 hectares in Sabah as shown in Figure 2.7. The mangrove area available as stated in the figure includes both reserved forest and state land shown in Table 2.4. As from the table, Sabah has the largest mangrove plants area, followed by Sarawak and Perak. Both illustrations show that Malaysia has a total of 629,038 hectares of mangrove plants land available (Omar, Husin and Parlan, 2020). One hectare of mangrove forests can adsorb 42 million tons of carbon in the air or, in other words, the amount of carbon gas emitted from 25 million cars every year. Thus, it is a good carbon source to synthesize activated carbon (Hamid, 2008).

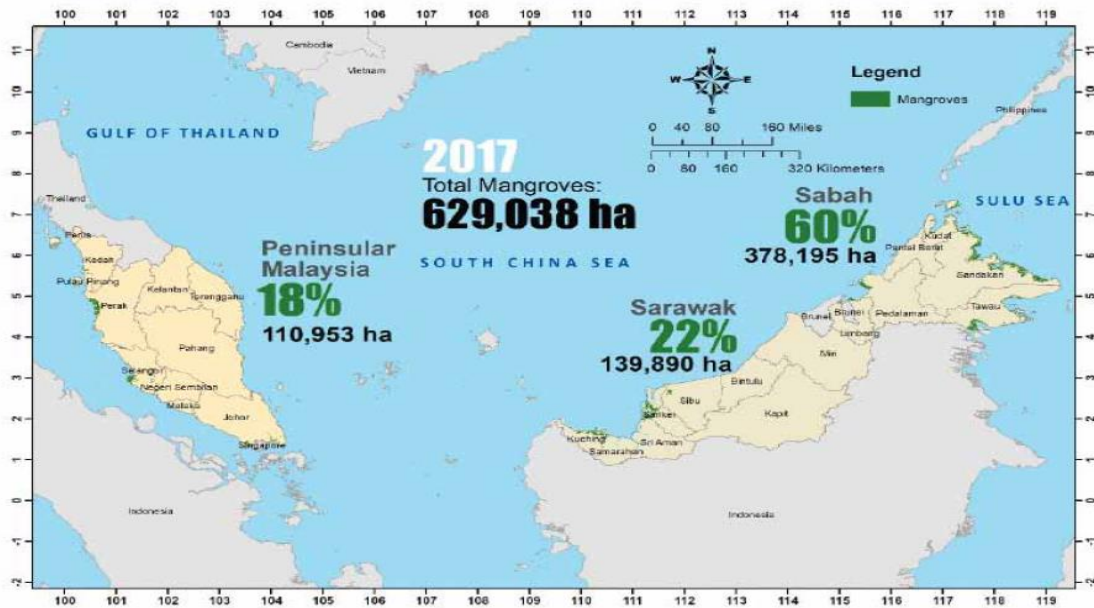


Figure 2.7 Area where mangrove forest can be found in Malaysia in 2017 (Omar, Husin and Parlan, 2020).

Table 2.4 Amount of mangrove forest available in each state of Malaysia in 2017 (Omar, Husin and Parlan, 2020).

State	Total (Hectare)
Perlis	49
Kedah	7725
Penang	1967
Perak	44,990
Selangor	20,853
Negeri Sembilan	1557
Melaka	1241
Johor	26,818
Pahang	3759
Terengganu	1571
Kelantan	422
Sabah	378,195
Sarawak	139,890
TOTAL	629,038

2.3 Adsorption Isotherm Model

The pore characteristics related to the activated carbon are obtained from the gas adsorption/desorption isotherm using the Brunauer–Emmett–Teller (BET) method.

The six categories of adsorption/desorption isotherms approved by the International

Union of Pure and Applied Chemistry (IUPAC) are depicted in Figure 2.8 (Nishi and Inagaki, 2016).

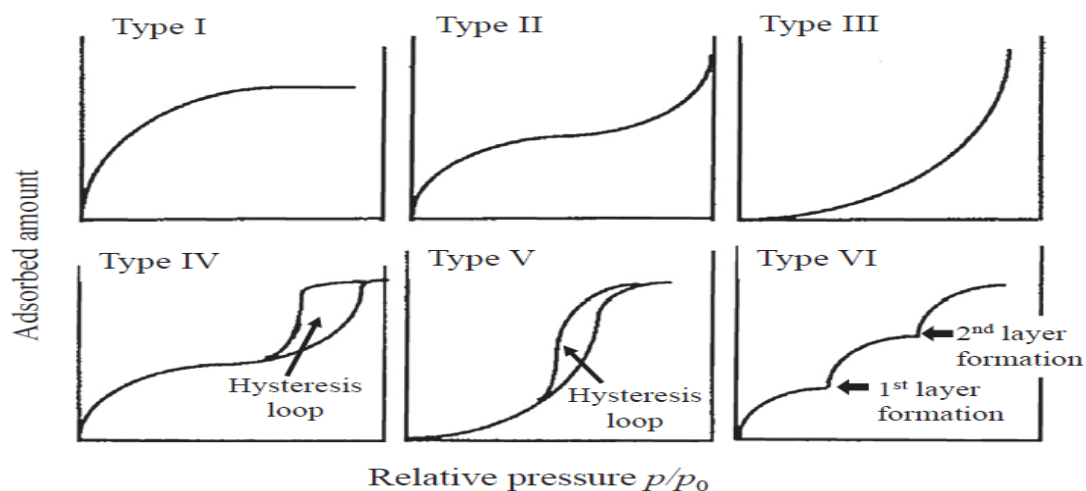


Figure 2.8 Types of isotherms defined by IUPAC (Nishi and Inagaki, 2016).

According to the figure, Type I is a typical microporous isotherm in which adsorption occurs rapidly and significantly up to a relative pressure p/p_0 of 0.1, with the adsorption process reaching equilibrium at p/p_0 of around 0.5. Type II displays monolayer adsorption followed by multilayer adsorption (Nishi and Inagaki, 2016). Type I and Type II isotherms are commonly seen on weak interactive carbon compounds to gas. The isotherm Type III reflects the intermolecular attractive interaction to adsorb gas particles, but without a full surface monolayer like Type IV. The Type IV is a typical isotherm for mesoporous materials that exists between adsorption and desorption curves with substantial hysteresis. Type V is next an extension of Type III, whereby the residual adsorbate condenses in the pore, due to the incomplete monolayer adsorption. Type VI is an adsorption on a highly uniform surface with a gradual isothermal layer-by-layer structure.

Adsorption equilibrium occurs when the concentration of adsorbate adsorbed from the wastewater become constant, and the adsorption isotherm is an interrelationship at this point. The adsorption isotherm is used to estimate various

adsorption parameters, such as maximum adsorption capacity and heterogeneity. Numerous existing adsorption isotherm models can be explored, including Langmuir, Freundlich, Temkin, Hill, Toth, and Redlich-Peterson. Among these isotherm models, Langmuir and Freundlich are the most widely known models applied by Foo and Hameed (2012b, 2012a), Rozaini *et al.* (2010), Salihi *et al.* (2018), Wan and Li (2018) and Wang *et al.* (2011). The correlation of equilibrium analysis is needed for both practical design and a fundamental understanding of adsorption systems.

The appropriateness of the isotherm model is always assessed using correlation coefficient (R^2) as the error analysis. In most cases, the best fit of a graph is chosen based on the comparison of R^2 values to unity (1.0). Nevertheless, in actual practice, the best fit of a graph with R^2 is rarely very close to 1.0 because there is always some degree of mistake caused by the experiment. Thus, it is recommended that a good fit a linear graph with successive R^2 values greater than 0.9 is acceptable. In spite of the fact that the performance of the model is dependent on R^2 , it can only be used as a source of reference rather than the primary indicator to determine the biases of the model because when two models have an approximate value of R^2 , the model with a lower R^2 might appear to fit better to experiment data after being implemented to non-linear form.

Most of the time, Langmuir isotherm model has a better fit in the linearized equation compared to Freundlich. According to Foo and Hameed (2012b, 2012a), Salihi *et al.* (2018), Wan and Li (2018) and Wang *et al.* (2011), Langmuir isotherm indicates monolayer adsorption whereby the adsorption can occur only at a finite number of localized sites that are identical and equivalent. It also suggests that the adsorption of heavy metal and dye onto activated carbon possesses equal enthalpy and

activation energy as the interaction between the adsorbate particles is neglected, and the energy distribution between the activated carbon is uniform.

On the other hand, experimental data of adsorption of copper (II) ions onto mangrove bark activated carbon in Rozaini *et al.* (2010) has proven to fit the Freundlich isotherm model. It is stated that Freundlich isotherm model describes multilayer adsorption and heterogeneous heat distribution due to the binding sites are not equivalent.

2.4 Adsorption Kinetics Model

The adsorption process is illustrated as a series of stages. The first step is the mass transfer of the fluid phase to the activated carbon particle surface across the external boundary layer film surrounding the outside of the particle. The second step is a rapid adsorption process at individual site on the adsorbent surface and the energy depends on the binding process (physical or chemical adsorption). Lastly, the third step is the diffusion of the adsorbate molecules to an adsorption site either by a pore diffusion process through the liquid-filled pores or by a solid surface diffusion mechanism. Overall, the rate-limiting step of the adsorption process will be one or any combination of these steps. Adsorption kinetics models are proposed to determine the potential rate-limiting step. The adsorption kinetics models that were used are pseudo-first-order (PFO), pseudo-second-order (PSO) model, Elovich and intra-particles.

The choice and appropriateness of the kinetics model are always assessed using correlation coefficient (R^2) and normalized standard deviation of adsorption capacity, Δq (%) as the error indicator as shown in Eq. 2.6. From the studies, pseudo-second-order (PSO) kinetics model is found to have a better fit than pseudo-first-order (PFO) for adsorption process (Alslaibi *et al.*, 2014; Aydin *et al.*, 2008; Chen *et al.*,

2011; Foo and Hameed, 2012b, 2012a; Rozaini *et al.*, 2010; Salihi *et al.*, 2018; Wan and Li, 2018; Wang *et al.*, 2011).

$$\Delta q(\%) = \sqrt{\frac{(q_{exp} - q_{cal})^2}{q_{exp} \cdot n - 1}} \quad 2.6$$

The best fit of PSO model reveals that the adsorption mechanism is more likely to be the rate-limiting step than the mass transfer of the fluid on activated carbon. Furthermore, PSO also suggests that strong and irreversible bonding (ionic and hydrogen bonding) within the adsorbent surface and adsorbate molecules is involved in the binding action, and the adsorption involves valency forces through electrons sharing between the hydrophilic site of activated carbon and adsorbate cation (Wang *et al.*, 2011; Foo and Hameed, 2012b; Salihi, Kutty and Ismail, 2018). On the other hands, if the kinetic model best fits pseudo-first order kinetic model, the adsorption more favors toward physisorption as the binding action, involving the weak and reversible Van der Waals force within the adsorbent surface and adsorbate molecules (Pourhakkak *et al.*, 2021).

2.5 Factor Affecting the Adsorption Performance

Adsorption performance of an activated carbon is commonly represented by a term called maximum adsorption capacity, Q_{max} which represents the amount of adsorbate adsorbed per unit mass of adsorbent used. Several studies have demonstrated that contact time, initial adsorbate solution concentration, temperature and pH of adsorbate solution and adsorbent dosage are the crucial parameters that will affect the adsorption efficiency of activated carbon (Alslaibi *et al.*, 2014; Aydin *et al.*, 2008; Chen *et al.*, 2011; Foo and Hameed, 2012b, 2012a; Ghaedi *et al.*, 2015; Marda and Astuti, 2017; Rozaini *et al.*, 2010; Salihi *et al.*, 2018; Wan and Li, 2018; Wang *et al.*, 2011).

2.5.1 Effect of Contact time

Based on Alslaibi *et al.* (2014) and Salihi *et al.* (2018), it was agreed that the adsorption is very rapid at the beginning stage. The adsorption capacity and adsorbate removal efficiency increased sharply and the slope of the curve at initial stage is the steepest. This phenomenon was predicted based on the availability of many surface sites for adsorption at the beginning. When times passed, because of the repulsion between the solute molecules of the adsorbate and the bulk phases, the remaining surface sites became more difficult to occupy as the reaction progresses. As equilibrium approached, the surface sites available was progressively reduced.

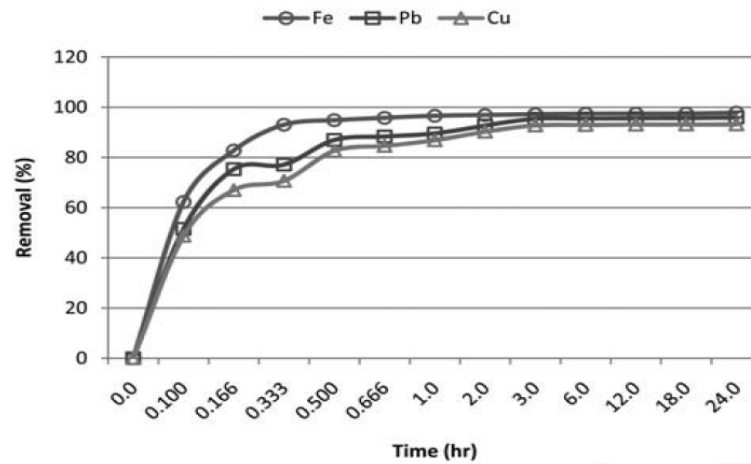


Figure 2.9 Effect of contact time on removal efficiency of Fe²⁺, Pb²⁺ and Cu²⁺ ions onto olive stone activated carbon (Alslaibi *et al.*, 2014).

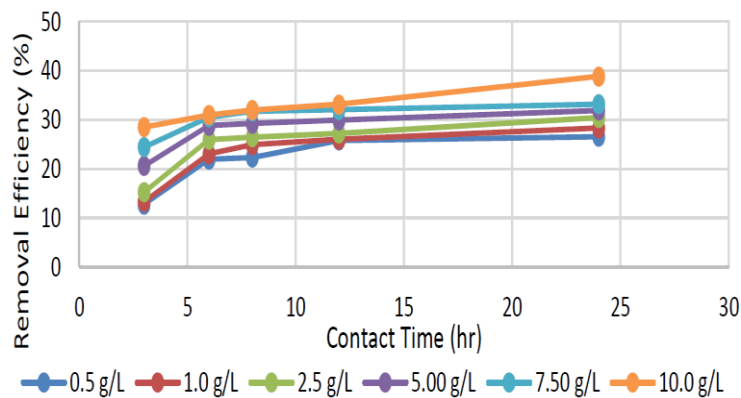


Figure 2.10 Effect of contact time on removal efficiency of Cu (II) ions at different initial concentration onto sugarcane bagasse activated carbon (Salihi, Kutty and Ismail, 2018).